Academic Journal of Science and Technology
ISSN: 2771-3032 | Vol. 4, No. 1, 2022

Signal Vector Design for Quadrature Index Modulation

Fuchun Huang

Guangzhou College of Commerce, Guangzhou 510700, China

Abstract: In this paper, we propose a new technique of quadrature index modulation with signal vector design (QIM-SSD), which can directly transmit a three-dimensional (3D) constellation symbol and expand an antenna index (AI) bit. The basic principle of QIM-SSD is as follows: two components of a mapped 3D signal symbol are first modulated on the upper and lower parts of transmit antennas (TAs) by two specific AI vectors with two blocks of AI bits, respectively, resulting in a space vector symbol. The remaining one component is modulated on one TA activated by the specific AI vector with one block of AI bits, then forming another space vector symbol. Furthermore, based on the resulted two space vector symbols, an additional bit is used to determine the real and imaginary parts of a complex transmit vector. The research of this paper is summarized as follows: firstly, the system model of QIM-SSD is introduced in detail. Then, the minimum Euclidean distance and the average bit error probability (BEP) are analyzed. With assumption of perfect channel estimation and maximum likelihood (ML) detection, simulation results demonstrate that the average BEP performance of QIM-SSD is better than that of the conventional QIM with three dimensional constellation and QSM at the same spectral efficiency by MATLAB simulator.

Keywords: Antenna index, 3D constellation, Euclidean distance, The real and imaginary parts of a complex transmit vector.

1. Introduction

Index modulation (IM), which exploits multiple index domains used to carry additional information, has been viewed as a potential key technology to improve the spectral efficiency (SE) and enhance the reliability of wireless communication. In [1], Quadrature space modulation (QSM) extends the spatial domain with the transmit antennas (TAs) to the in-phase and quadrature spatial dimensions that modulate the real and imaginary parts of the mapped symbol (e.g., quadrature amplitude modulation/phase shift modulation (QAM/PSK)). Consequently, QSM can achieve the additional information bits of twofold base-two logarithm of the number of TAs. In order to make use of the idle TAs, based on the in-phase and quadrature dimensions, a lot of works on generalization of QSM (GQSM) [2-4] have been developed to achieve more additional index bits by increasing the active AI combinations. However, the additional index bits that GQSM achieves are increased at the cost of the detection complexity that will be relatively increased with the increasing of active TAs. To effectively utilize the idle antennas, from the perspective of developing signal constellation, quadrature index modulation with three dimension (3D) constellation (QIM-TDC) [5] is proposed to transmit two components of a 3D symbol by using two active TAs in the in-phase dimension and to transmit the remaining one by using one active TA in the quadrature dimension, respectively. Consequently, compared with QSM, QIM-TDC improves not only the squared minimum Euclidean distance (MED) but also the additional index bits with the increasing of TAs.

However, it can be observed that QIM-TDC does not make full use of the difference between the real part and the imaginary part of the transmit vector. Based on this issue, a new design, called quadrature index modulation with spatial signal design (QIM-SSD), which further exploit the spatial domain for additional index information, is proposed to design the transmit vector to increase the SE and enhance the reliability of communication. Specifically, one spatial vector symbol is obtained by modulating the two components of the mapped 3D signal constellation point (CP) on two active TAs, and another one is obtained by modulating the one component of the mapped 3D signal CP on one active TAs. Then, with the aid of the one bit, the two spatial vector symbols are determined as the real and imaginary parts of the transmit vector. Furthermore, the squared MEDs of QIM-SSD are provided and compared with that of the QSM and QIM-TDC systems. Finally, simulation results demonstrate that QIM-SSD outperforms the QSM and QIM-TDC systems in terms of bit error rate (BER) performance.

2. The Proposed QIM-SSD

2.1. System Model

Considering the QIM-SSD system with the number of N_t TAs, as depicted in Fig.1. In our proposed QIM-SSD system, the transmit vector symbol and the input bits sequence is denoted by $\mathbf{X}$ and $\mathbf{m}$, respectively.

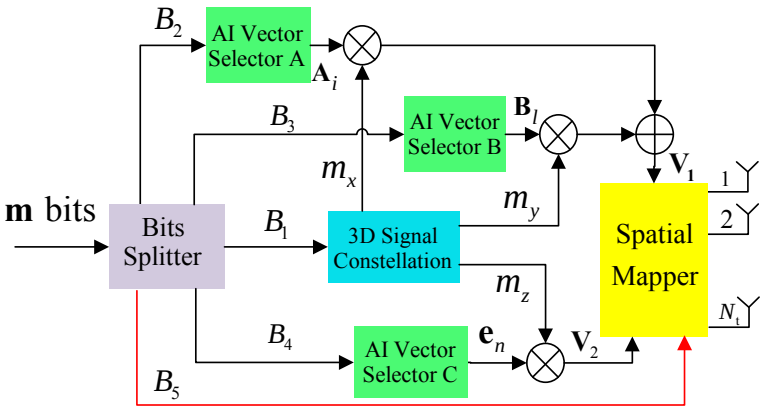

Figure 1. System Model of QIM-SSD

As depicted in Fig. 1, the input information bits $\mathbf{m}$ are divided into five blocks: B_1, B_2, B_3, B_4, B_5. For the first block of B_1, containing $\log_2(M)$ bits, it is mapped into a M-ary 3D CP symbol $s_\lambda(m_x, m_y, m_z)$, $\lambda \in \{1, \mathrm{L}, M\}$ from the 3D signal constellation [5] denoted by $\Omega = \{s_1, \mathrm{L}, s_M\}$, e.g., 16-ary 3DCII: $\Omega = \{(\pm 1, \pm 1, \pm 2), (\pm 1, \pm 2, \pm 1)\}$. Through three antenna index (AI) vector selectors: A, B, C□three blocks of B_2, B_3, B_4 information bits are mapped into three AI vectors from the AI vector sets: $\mathfrak{v}$, $\boldsymbol{\kappa}$, $\mathbf{e}$, respectively. Specifically, in order to consider that three components (m_x, m_y, m_z) of the mapped $s_\lambda(m_x, m_y, m_z)$ are modulated by the three AI vectors simultaneously in a QIM-SSD symbol period without interference, the two components (m_x, m_y) are modulated on two different active TAs, and the component m_z is modulated on one active TA. The design rules of two spatial vectors symbol ($\mathbf{V}_1$, $\mathbf{V}_2$) for the in-phase or quadrature dimension are follow :

The design of the spatial vector symbol $\mathbf{V}_1 = m_x\mathbf{A}_i + m_y\mathbf{B}_l$.

The two block of B_2, containing $\log_2(N_t/2)$ bits, is used to select one AI vector $\mathbf{A}_i$, $i \in \{1, \cdots, N_t/2\}$ from the AI vector set $\mathfrak{v} = \{\mathbf{A}_1, \cdots, \mathbf{A}_{N_t/2}\}$; the block of B_3 containing $\log_2(N_t/2)$ bits, is used to select one AI vector $\mathbf{B}_l$ □ $l \in \{1, \cdots, N_t/2\}$ from the AI vector set $\boldsymbol{\kappa} = \{\mathbf{B}_1, \cdots, \mathbf{B}_{N_t/2}\}$. Then, the two AI vectors $\mathbf{A}_i$ and $\mathbf{B}_l$ respectively modulate the two components m_x, m_y of the mapped 3D symbol $s_\lambda(m_x, m_y, m_z)$, resulting in two spatial vector symbols: $m_x\mathbf{A}_i$ and $m_y\mathbf{B}_l$. To avoid mutual interference, $m_x\mathbf{A}_i$ and $m_y\mathbf{B}_l$ are transmitted on the upper and lower parts of TAs. Thus, a spatial vector symbol $\mathbf{V}_1 = \left[m_x\mathbf{A}_i \; m_y\mathbf{B}_l\right]^T$ is obtained as by combining $m_x\mathbf{A}_i$ with $m_y\mathbf{B}_l$, where $\mathbf{A}_i$ with $N_t/2\times 1$ dimensions represents a vector with a non-zero element equaling to 1 in the i-th row and is used to make the i-th TA be in active state, $\mathbf{B}_l$ with $N_t/2\times 1$ dimensions represents a vector with a non-zero element equaling to 1 in the ℓ-th row and is used to make the $N_t/2+\ell$-th TA be in active state.

The design of the spatial vector symbol $\mathbf{V}_2 = m_z \cdot \mathbf{e}_n$

For the last block of B_4, containing $\log_2(N_t)$ bits, it is used to selected a AI vector $\mathbf{e}_n$ with $N_t \times 1$ dimensions from the AI vector set $\mathbf{e} = \{\mathbf{e}_1, \cdots, \mathbf{e}_{N_t}\}$, where $n \in \{1, \cdots, N_t\}$. Then, the selected AI vector $\mathbf{e}_n$ is used to modulate the component m_z of the the mapped 3D symbol $s_\lambda(m_x, m_y, m_z)$, resulting in a spatial vector symbol $\mathbf{V}_2 = m_z \cdot \mathbf{e}_n$, where $\mathbf{e}_n$ represents a vector with a non-zero element equaling to 1 the n-th row and is used to make the n-th TA be in active state.

Here, to further explain the three AI vector sets, the following examples are provided, assumed that $N_t = 4$,

$$\mathfrak{v} = \begin{bmatrix} 1 & 0 \\ 0 & 1 \end{bmatrix}, \quad \boldsymbol{\kappa} = \begin{bmatrix} 1 & 0 \\ 0 & 1 \end{bmatrix}, \quad \mathbf{e} = \begin{bmatrix} 1 & 0 & 0 & 0 \\ 0 & 1 & 0 & 0 \\ 0 & 0 & 1 & 0 \\ 0 & 0 & 0 & 1 \end{bmatrix} \quad (1)$$

In order to further transmit more additional information bits, we use one index bit to determine the real part and the imaginary part of the complex transmit vector $\mathbf{X}$. Specifically, when the block of B_5=0, the vector symbol $\mathbf{V}_1$ is considered as the real part of the complex vector $\mathbf{X}$, while the vector symbol $\mathbf{V}_2$ is considered as the imaginary part of the complex vector $\mathbf{X}$. Otherwise, the vector symbol $\mathbf{V}_1$ is considered as the imaginary part of the complex vector $\mathbf{X}$, the vector symbol $\mathbf{V}_2$ is considered as the real part of the

complex vector $\mathbf{X}$. Consequently, with the determining of the block B_5, the complex vector $\mathbf{X}$ is obtained as

$$\mathbf{X}=\begin{cases}\mu\left(\mathbf{V}_1+j\cdot\mathbf{V}_2\right), & B_5=0\\ \mu\left(\mathbf{V}_2+j\cdot\mathbf{V}_1,\right), & B_5=1\end{cases}$$
$$=\begin{cases}\mu\left(m_x\mathbf{A}_i+m_y\mathbf{B}_l+jm_z\mathbf{e}_n\right), & B_5=0\\ \mu\left[m_z\mathbf{e}_n+j(m_x\mathbf{A}_i+m_y\mathbf{B}_l)\right], & B_5=1\end{cases} \quad (2)$$

where, $\mu=1/E_{\text{av}}$, E_{av} denotes the average energy of each complex transmit vector $\mathbf{X}$.

To further explain the working principle of forming the complex transmit vector $\mathbf{X}$, examples for which are given in following Table I, assumed that $N_{\text{t}}=4$, $B_1\rightarrow s_\lambda(m_x,m_y,m_z)$, and three AI vector sets are obtained according to (1).

B_2	B_3	B_4	B_5	$\mathbf{X}$
0	0	0 0	0	$[m_x+jm_z,0,m_y,0]^T$
0	1	0 1	0	$[m_x, jm_z,0,m_y]^T$
1	0	1 0	0	$[0,m_x, m_y+jm_z ,0]^T$
1	1	1 1	0	$[0,m_x, 0, m_y+jm_z]^T$
0	0	0 0	1	$[jm_x+m_z,0,jm_y,0]^T$
0	1	0 1	1	$[jm_x, m_z,0,jm_y]^T$
1	0	1 0	1	$[0,jm_x, jm_y+m_z ,0]^T$
1	1	1 1	1	$[0,jm_x,0 , jm_y+m_z]^T$

2.2. Receiver and Detection

At the receiver, after transmitting the complex transmit vector $\mathbf{X}$ over the MIMO channel matrix $\mathbf{H}$ with an additive white Gaussian noise (AWGN) vector $\mathbf{N}$, the receive signal vector can be expressed as

$$\mathbf{Y}=\mathbf{HX}+\mathbf{N} \quad (3)$$

where $\mathbf{Y}\in C^{N_{\text{r}}\times 1}$, $\mathbf{H}\in C^{N_{\text{r}}\times N_{\text{t}}}$ is a Rayleigh-fading channel matrix, whose each entry is assumed to be an independent and identically distributed complex Gaussian random variable with $CN(0,1)$. $\mathbf{N}\in C^{N_{\text{r}}\times 1}$ is the Gaussian white noise vector with zero-mean and σ^2 covariance, i.e., $CN(0,\sigma^2\mathbf{I}_{N_{\text{r}}})$.

Under the conditions of the ideal channel estimation and maximum likelihood (ML) detection, for better detection of the original information bits, the algorithm of the ML decoder is given by

$$[\hat{i},\hat{l},\hat{n},\hat{B}_5,\hat{s}]=\arg\min_{i,l,n,s,B_5}\left\|\mathbf{Y}-\mathbf{HX}\right\|^2 \quad (4)$$

where $\hat{s}$ denotes the estimate of the 3D mapped symbol s. $\hat{i}$, $\hat{l}$, $\hat{n}$ denote the estimated index number of the AI vectors $\mathbf{A}_i,\mathbf{B}_l,\mathbf{e}_n$. $\hat{B}_5$ denotes the estimate of the block B_5.

3. Performance Analysis

3.1. Bit Error Probability

In this paper, the channel state information is assumed to be perfect, and the estimated transmit vector of the normalized transmit vector $\mathbf{X}$ is expressed as $\hat{\mathbf{X}}$.

Based on the union bound technique [6], the average PEP can be derived by

$$APEP\le\frac{1}{\mathbf{m}2^{\mathbf{m}}}\sum_{\mathbf{X}}\sum_{\hat{\mathbf{X}}}PEP(\mathbf{X}\rightarrow\hat{\mathbf{X}})\cdot e(\mathbf{X}\rightarrow\hat{\mathbf{X}}) \quad (5)$$

where $e(\mathbf{X}\rightarrow\hat{\mathbf{X}})$ is the total number of erroneous bits.

Based on the moment generating function [6], the average pairwise error probability (PEP) conditioned on $\mathbf{H}$ can be calculated by

$$PEP(\mathbf{X}\rightarrow\hat{\mathbf{X}})=E_{\mathbf{H}}\left\{Q\left(\sqrt{\frac{\left\|\mathbf{H}\left(\mathbf{X}-\hat{\mathbf{X}}\right)\right\|^2}{2N_0}}\right)\right\}=\frac{1}{\pi}E_{\mathbf{H}}\left\{\int_0^{\frac{\pi}{2}}\frac{\left\|\mathbf{H}\left(\mathbf{X}-\hat{\mathbf{X}}\right)\right\|^2}{4N_0\sin^2\theta}d\theta\right\}$$
$$=\frac{1}{\pi}\int_0^{\frac{\pi}{2}}\left(\frac{\sin^2\theta}{\sin^2\theta+\frac{d^2_{\mathbf{X},\min}}{4N_0}}\right)^{N_{\text{r}}}d\theta=\left(\frac{1-\eta}{2}\right)^{N_{\text{r}}}\sum_{k=0}^{N_{\text{r}}-1}C_k^{N_{\text{r}}-1+k}\left(\frac{1+\eta}{2}\right)^k \quad (6)$$

where $Q(\cdot)$ denotes the Gaussian Q function, $\eta=\sqrt{d^2_{\mathbf{X},\min}/\left(4N_0+d^2_{\mathbf{X},\min}\right)}$, $d^2_{\mathbf{X},\min}=\min_{\lambda\neq\lambda'}\left\|\mathbf{X}_\lambda-\hat{\mathbf{X}}_{\lambda'}\right\|^2$.

Thus, the average PEP will be derived by substituting the E.q. (6) into the E.q. (5). Moreover, it can be observed from the E.q. (6), when the number of receive antennas is fixed, the larger the squared MED is, the smaller it is, and the better the asymptotic system performance is.

3.2. Squared Minimum Euclidean Distance

Based on the above mentioned design and analysis, the squared MED $d^2_{\mathbf{X},\min}$ between the transmit vectors for the QIM-SSD may be calculated by

$$d^2_{\mathbf{X},\min}=\min_{\lambda\neq\lambda'}\left\{\left\|\mathbf{X}_\lambda-\hat{\mathbf{X}}_{\lambda'}\right\|^2\right\} \quad (7)$$

Then, according to the E.q.(7), the squared MEDs $d^2_{\mathbf{X},\min}$ are listed in Table I and compared with that of both QSM and QIM-TDC at different SEs, where pTXmb denotes transmitting m bits in each time slot with pTAs and Signal C. is Abbreviation of Signal Constellation.

Table 2. Comparison of the squared MED at different SEs and TAs.

	4TX8b		4TX9b		8TX11b		8TX12b	
	Signal C.	$d^2_{\mathbf{X},\min}$	Signal C.	$d^2_{\mathbf{X},\min}$	Signal C.	$d^2_{\mathbf{X},\min}$	Signal C.	$d^2_{\mathbf{X},\min}$
QSM	16QAM	2/10	32QAM	2/20	32QAM	2/20	64QAM	2/42
QIM-TDC	16-3DCII	2/6	32-3DCII	2/8	16-3DCII	2/6	32-3DCII	2/8
QIM-SSD	8-3DCI	2/3	16-3DCII	2/6	8-3DCII	2/3	16-3DCII	2/6

It can be observed from Table II that the squared MEDs $d^2_{\mathbf{X},\min}$ of the QIM-SSD have the larger value than the QSM and QIM-TDC systems at the same SE. Furthermore, at high signal noise ratio (SNR), due to that the asymptotic performance is mainly determined by the worst-case PEP, which corresponds to the squared MED between the transmit vectors. According to the analysis of Table II, in high SNR region, the BER performance of the presented QIM-SSD system is more reliable than both QSM and QIM-TDC in wireless communication network.

4. Results and Discussion

In this section, the BER vs SNR performance for the QIM-SSD by implementing the ML detector at the receiver is numerically expounded and compared with that of the QSM and QIM-TDC at the same spectral efficiency and TAs. Based on the analysis of Table II, simulation results using Monte Carlo for QIM-SSD are provided to verify the advantage of QIM-SSD with $[N_t, N_r] = [4, 4]$. In our simulation results, the channel state information is assumed to be perfect at the receiver.

In Fig. 2, the BER vs SNR curves of QIM-SSD are depicted and compared with that of QSM and QIM-TDC at different SEs (4TX8b and 4TX9b b/s/Hz) and TAs. At the scenario of 4TX8b, since the QIM-SSD achieves one more extra index bit than that the QIM-TDC achieve, the QIM-SSD only transmit the 8-ary 3DC signal CP symbol, but the QIM-TDC and QSM need to transmit the 16-ary 3DCII and the 16QAM signal CP symbols, respectively. Thus, according to the analysis of Table II, the squared MED (e.g., 2/3) of QIM-SSD is bigger than that (e.g., 2/6, 2/10) of both QIM-TDC and QSM. So that the QIM-SSD achieves better BER performance than the QIM-TDC and QSM. It can be observed from Fig. 2 that 1.8 dB SNR gain over QIM-TDC, 5 dB SNR gain over QSM are achieved for QIM-SSD at the BER value of 10^{-4}. Similarly, the QIM-SSD with 16-ary 3DCII has bigger squared MED than the QIM-TDC with 32-ary 3DCII and the QSM with 32QSM, so as to improve the BER performance.

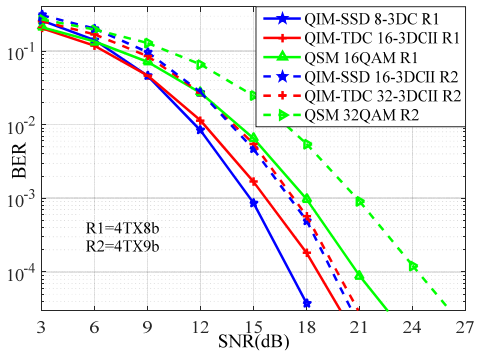

Figure 1. BER performance comparison of QIM-SSD with the QIM-TDC and QSM at 4TX8b and 4TX9b.

5. Conclusion

Based on the advantages and characteristics of 3D constellation mapping, a new design, called QIM-SSD, is proposed to enhance the spectral efficiency and the reliability of the wireless communication system. Furthermore, the squared MED comparisons between QIM-SSD and the QIM-TDC and QSM systems are provided. Under the conditions of ideal channel estimation and maximum likelihood detection, simulation results demonstrate that the proposed QIM-SSD achieves the better BER performance. In a word, the exploiting of the spatial domain and the increasing of the squared MED are good means to further improve the BER performance of mobile communication.

References

[1] R. MESLEH, S. S. IKKI, H. M. AGGOUNE (2015). Quadrature spatial modulation [J]. IEEE Transactions on Vehicular Technology, vol. 64, no.6, p. 2738-2742.

[2] K. Gunde and A. Sundru (2021). Modified generalized quadrature spatial modulation performance over Nakagami-m fading channel, Int J. Commun. Syst., vol. 34, no. 16, 2021.

[3] J. Li, S. Dang, and et al. (2021). Generalized Quadrature Spatial Modulation and Its Application to Vehicular Networks With NOMA, IEEE Trans. Intell. Transp. Syst., vol. 22, no. 7, p. 4030–4039.

[4] L.Wang (2021). Generalized Quadrature Space-Frequency Index Modulation for MIMO-OFDM Systems, IEEE Trans. Commun., vol. 69, no. 9, p.6375–6389.

[5] F. Huang, X. Liu, and et al (2019). Quadrature Index Modulation with Three-Dimension Constellation, IEEE Access, vol. 7, p. 182335–182347, 2019.

[6] M. SIMON, M. ALOUINI (2005). Digital communication over fading channels [M]. Hoboken, New Jersey: Wiley-IEEE Press, p.758-795.